Received: 22 September 2023 | Accepted: 4 December 2023

DOI: 10.1111/imm.13742

ORIGINAL ARTICLE

immunology
Insights into immunity in health and disease

Idiotopes of antibodies against HIV-1 CD4-induced epitope shared with those against microorganisms

Shashwata Biswas[1] | **Takeo Kuwata**[1] | **Soichiro Yamauchi**[2] | **Kyo Okazaki**[2] | **Yu Kaku**[1] | **Md Zahid Hasan**[1] | **Hiroshi Morioka**[2] | **Shuzo Matsushita**[1]

[1]Division of Clinical Retrovirology, Joint Research Center for Human Retrovirus Infection, Kumamoto University, Kumamoto, Japan

[2]Department of Analytical and Biophysical Chemistry, Faculty of Medical and Pharmaceutical Sciences, Kumamoto University, Kumamoto, Japan

Correspondence
Takeo Kuwata and Shuzo Matsushita, Division of Clinical Retrovirology, Joint Research Center for Human Retrovirus Infection, Kumamoto University, Kumamoto 860-0811, Japan.
Email: tkuwata@kumamoto-u.ac.jp and shuzo@kumamoto-u.ac.jp

Funding information
Japan Agency for Medical Research and Development, Grant/Award Numbers: JP20fk0410025h0002, JP21fk0410025h0003, JP22fk0410054h0001, JP23fk0410054h0002; JSPS KAKENHI, Grant/Award Numbers: 18H0285400, 21H02970

Abstract

Induction of antibodies (Abs) against the conformational CD4-induced (CD4i) epitope is frequent in HIV-1 infection. However, the mechanism of development of anti-CD4i Abs is unclear. We used anti-idiotypic (aID) monoclonal Abs (mAbs) of anti-CD4i mAbs to isolate anti-CD4i mAbs from infected subjects and track the causative antigens. One anti-aID mAb sorted from infected subjects by aID mAbs had the characteristics of anti-CD4i Abs, including IGHV1-69 usage and ability to bind to HIV-1 Env enhanced by sCD4. Critical amino acid sequences for the binding of six anti-aID mAbs, with shared idiotope to anti-CD4i mAbs, were analysed by phage display. The identified amino acid sequences showed similarity to proteins from human microbiota and infectious agents. Peptides synthesized from *Caudoviricetes sp* and *Vibrio vulnificus* based on the identified sequences were reactive to most anti-aID and some anti-CD4i mAbs. These results suggest that anti-CD4i Abs may evolve from B cells primed by microorganisms.

KEYWORDS
AIDS, antibodies, antigens/peptides/epitopes

INTRODUCTION

Since its discovery in 1983 [1], numerous attempts to develop a protective vaccine for human that induces neutralising antibodies (Abs) against human immunodeficiency virus type 1 (HIV-1) have remained largely unsuccessful. Only the RV144 trial showed the significant decrease in HIV infection risk, and the Abs against the V2 region were identified as a correlate of reduced infection risk [2, 3]. The reasons behind the failure to develop an effective vaccine include the lack of correlates of protective immunity, presence of viral reservoirs in the form of provirus in various tissues, genetic variability of HIV-1, and inability to induce broadly reactive Ab responses [4]. The induction of broadly neutralising Abs is a key factor for the development of an effective vaccine, but it is challenging to develop vaccines against HIV-1 [5]. Instead of broadly neutralising Abs, which are difficult to induce by vaccination, the induction of non-neutralising Abs is an alternative option in vaccine development [6]. Non-neutralising Abs are relatively easy to induce by immunisation and they mediate Fc-dependent functions, such as antibody-dependent cellular cytotoxicity (ADCC).

Shuzo Matsushita is the lead contact.

An important epitope on HIV-1 Env is the CD4-induced (CD4i) epitope, which contains the co-receptor binding site. The interaction between CD4 on the host cell surface and the CD4 binding site (CD4bs) on the gp120 of Env initiates conformational changes of gp120 that expose the co-receptor binding site on the Env trimer by the rearrangement of the V1, V2 and V3 loops [7–11]. Finally, gp41 mediated membrane fusion occurs after the binding of chemokine receptors to the bridging sheet region on gp120 [12–15]. The bridging sheet is comprised of two double-stranded β-sheets formed with β2 and β3 at the stem of the V1/V2 loops and β20 and β21 at the C4 region [11–16]. These β sheets are highly conserved among various HIV-1 strains because the structure and amino acid (aa) sequence of this region are critical for the interaction with CCR5 [17, 18]. Hence, Anti-CD4i single-chain variable fragments, which consist of variable regions of antibody, bind and inhibit most HIV-1 strains from various clades, although only the small fragments of antibody are accessible to CD4i epitope [19]. In addition, anti-CD4i Abs mediate ADCC against various HIV-1 strains, especially in the presence of CD4-mimetic compound [20–23].

In HIV-1 infection, Abs against the CD4i epitope—the conformational epitope consisting of β sheets from the V1/V2 loops and C4 region—are frequently observed; however, what triggers the induction of the anti-CD4i Abs remains unclear. To examine the possibility of priming of B cell precursors against CD4i epitope by antigens other than HIV-1, we obtained anti-idiotypic (aID) monoclonal Abs (mAbs) that may mimic the target antigen structures [24] and therefore provide us with the opportunity to search for antigens with common structures. The identification of antigens that prime anti-CD4i Abs may help in designing immunogens for future vaccine studies.

We previously reported several anti-CD4i mAbs isolated from an elite controller [19, 25]. Binding site analysis revealed that the anti-CD4i mAbs—4E9C and 916B2—have highly specific binding to the β20/β21 and β2/β3 sheets, respectively [19]. To isolate aID mAbs that mimic the antigenic structures, we immunised mice with 4E9C and 916B2, isolated antigen-specific B cells by single-cell sorting, and screened the isolated mAbs for specificity using several methods to select appropriate candidates. The selected aID mAbs were used as probes to isolate anti-aID mAbs from HIV-1-infected subjects. Analysis of anti-aID mAbs indicated that a fraction of anti-CD4i Abs may be primed by antigens from human microbiome and infectious agents.

METHODS

Study subjects

This study received ethical approval from the Ethics Committee for Clinical Research and Advanced Medical Technology at the Kumamoto University (Approval No. 1637). All participants gave written, informed consent prior to inclusion.

Animals

This study was approved by the Committee of Animal Experimentation at Kumamoto University, and was conducted in strict accordance with the Guidelines of the Japanese Pharmacological Society for the Care and Use of Laboratory Animals.

Mouse immunisation and collection of spleen cells

BALB/c mice were immunised by 4E9C and 916B2 mAbs, and 100 μg immunoglobulin (IgG) was administered to each mouse by intramuscular (i.m.) injection on days 0, 14, 28, 42 and 56. Mice were sacrificed on day 61, and spleen cells were collected in Ficoll-Paque™ Plus (GE Healthcare, Cat#17–1440-03) after straining using a 100-μm strainer. Cells were stored at −80°C in serum-free freezing medium Bambanker (GC Lymphotec Inc., Cat# CS-04-001).

Sorting aID-expressing mouse spleen cells

Approximately 10^7 frozen cells were washed in Dulbecco's phosphate buffered saline (D-PBS) (Wako, Cat#045–29 795) and B cells were magnetically separated by using a Mojosort™ Mouse Pan B Cell Isolation Kit (Biolegend, Cat#480052). The separated cells (CD90.2, CD11c, Gr-1, CD49b and TER-119/erythroid negative cells) were resuspended in 0.2% bovine serum albumin (BSA) (Nacalai tesque, Cat#01859–47) in PBS, blocked with 100 μg/mL Normal Human IgG (NHG) (Sigma-Aldrich, Cat#I2511-10MG) for 30 min and stained with biotinylated 4E9C and 916B2 at 10 μg/mL for 40 minutes. Following washing, Phycoerythrene (PE) anti-mouse IgG2ab (Miltenyi Biotec, Cat#130–117-787) and IgG1 (Miltenyi Biotec, Cat#130–119-585), Brilliant Violate (BV421) anti-mouse IgM (Biolegend, Cat#406517), Fluorescein isothiocyanate (FITC) anti-mouse CD19 (Biolegend, Cat#115505)

and Allophycocyanin (APC) streptavidin (Biolegend, Cat#405207) were added to the cell suspension at recommended volumes and incubated for 40 min. All incubations were carried out on ice. Cells were washed and subjected to single-cell sorting by a FACS Aria II (BD Biosciences) cell sorter using a 100-nm nozzle after adding 7AAD (BD Biosciences, Cat#559925). 7AAD-CD19+ IgM-IgG+ cells that bound to biotinylated anti-CD4i Abs (APC+) were sorted and single cells were collected in 96-well PCR plates, each well containing 5 μL of 50 μM guanidine thiocyanate (Invitrogen, Cat#AM9422) as a lysis agent. Plates containing the sorted cells were stored at −80°C until further use.

Sorting B cells from infected subjects' peripheral blood mononuclear cells (PBMCs)

PBMCs were isolated from infected subjects' blood samples by gradient centrifugation using Ficoll-Paque™ Plus. Cells were resuspended in mojosort buffer (Biolegend, Cat#480017) and allowed to react with recommended volumes of biotin CD3 monoclonal antibody (eBioscience, Cat#13–0038-82), biotin mouse anti-human CD8 (BD Biosciences, Cat#555365) and biotin CD14 monoclonal antibody (eBioscience, Cat#13–0149-82) for 15 min. Following wash, streptavidin nanobeads (Biolegend, Cat#480015) were added to the cell suspension and incubated for 15 min. After washing, unlabelled fraction of the cells (CD3-CD8-CD14-population) were collected using a Mojosort magnet (Biolegend, Cat#480019). Magnetically sorted cells were stained with BV 421 mouse anti-human IgG (BD Biosciences, Cat#562581) for 40 min. After washing, cells were blocked by 1 mg/mL of NHG for 30 minutes and biotinylated 4G8D and 9J6C aID mAbs were added at 20 μg/mL followed by incubation for 40 min. FITC anti-human CD19 (BioLegend, Cat#302206), APC/Cy7 anti-human IgM (BioLegend, Cat#314520), PE anti-human CD27 (BioLegend, Cat#356406) and APC streptavidin were added to cells after washing and incubated for 40 min. After a final wash, cells were stained with 7AAD. All incubations were carried out on ice in the dark. 7AAD-CD19 + IgM-IgG + CD27+ cells that bound to biotinylated aID mAb (APC+) were sorted.

Cloning of IgG variable region genes from mice

cDNA was synthesized by reverse transcription according to a previously described method [26, 27] using Superscript III reverse transcriptase (Invitrogen, Cat#18080085). IgG variable region genes were amplified from cDNA by nested PCR using hot star taq polymerase (Qiagen, Cat#203605). Purified DNA was inserted into pcDNA3.1 based human IgG heavy (pIgGH) and light chain (pKVA2) expression vectors by homologous recombination using Gibson assembly master mix (New England Biolabs, Cat#E2611). Plasmids were amplified by transforming top 10 chemically competent *Escherichia coli* (ThermoFisher Scientific, Cat#C404010) cultured in LB broth (Nacalai tesque, Cat#20068–75) and purified using plasmid extraction kit (Sigma-Aldrich, Cat#PLN350-1KT). Sanger sequencing was performed for the heavy and light chains of each sample using an AB3500XL (Applied Biosystems) sequencer. The nucleotide sequences of the IgGs and germline gene verification, framework, and CDR mapping were performed as previously described [28] using IMGT vquest [29].

Production and purification of mouse-human chimeric aID mAbs

Heavy and light chain plasmids were co-transfected using TransIT-LT1 transfection reagent (Mirusbio, Cat#-MIR2300) into Human Embryonic Kidney (HEK) 293 T cells maintained in Dulbecco's Modified Eagle's Medium (Nacalai tesque, Cat#08458–16) supplemented with 10% heat inactivated Fetal Bovine Serum (FBS; Sigma, Cat#173012) and after 48 h, IgG expression was checked and quantified by human IgG assay. First, 96-well polystyrene microtiter plates were coated with 100 μL (1:1000) goat anti-human IgG (γ chain specific) (Sigma-Aldrich, Cat#I3382) in carbonate bicarbonate buffer (CBB) pH 9.6 and incubated at 4°C overnight. After washing, culture supernatants and standards were added at three times serial dilution in ELISA buffer (0.03% Tween 20 and 1% FBS in PBS) and plates were incubated for 1 h at 37°C followed by another wash. Goat anti-human IgG (γ-chain specific) alkaline phosphatase conjugated secondary antibody (Sigma-Aldrich, Cat#A3150) was added (1:1000) to each well followed by incubation at 37°C for 1 h. After a final wash, phosphatase substrate solution (Sigma-Aldrich, Cat#S0942-200TAB) was added to each well. The optical density (OD) value was measured at 405 nm by a microplate reader (Bio-Rad). Sample concentrations were calculated from standard curve. aID mAbs from HEK 293 T cells were used for the screening of inhibitory properties. Selected mAbs were purified from stably IgG-expressing HEK 293A cells. Cells were cloned from colonies selected by G418 (1 mg/mL)

(Millipore, Cat#345812) and hygromycin B (150 μg/mL) (Nacalai tesque, Cat#07296) after transfection with heavy and light chain plasmids. Supernatants were collected every alternate day and purified by a HiTrap rProtein A FF Column (Cytiva, Cat#17508002). In short, IgG expressing supernatant was passed three times through the column with the help of a peristaltic pump and bound IgGs were eluted from the column using Glycine (Wako, Cat#077–00735)-HCl buffer pH 2.6 and collected in fraction collector tubes containing 1 M tris buffer pH 9.1 in sufficient volume to neutralise the pH of resultant fraction. All fractions were collected and dialyzed against PBS. After concentrating by PEG 6000 (Fujifilm, Cat#169–09125), the eluate was again dialyzed against PBS, filtered by 0.2 μm syringe filter and stored at −80°C until further use. 4G8D and 9J6C were also expressed in ExpiCHO-S cells (Gibco, Cat#A29127) maintained in ExpiCHO expression medium (Gibco, Cat#A29100-01) after transient transfection using ExpiFectamine™ CHO Transfection Kit (Gibco, Cat#A29129) and Optipro SFM (Gibco, Cat#12309–050). Expressed mAbs were purified using a HiTrap rProtein A FF Column as described above.

Production of recombinant IgGs from HIV-1-infected subjects

cDNA was synthesized by reverse transcription as previously described [28]. IgG variable region genes were amplified from cDNA by nested PCR. Purified DNA was inserted into pcDNA3.1 based human IgG heavy (pIgGH) and light chain (pKVA2 for kappa chain and pLSH for lambda chain) expression vectors by homologous recombination. Recombinant IgGs were expressed in HEK 293 T transfected supernatant and those with IGHV 1–69 germline usage were purified using Protein A spin column (Cosmo Bio Co. Ltd., Cat#APK-10A) for screening of binding activity and competitive binding inhibition analyses. The six selected anti-aID mAbs were purified from ExpiCHO-S cells.

Competitive binding inhibition assay by aID mAbs

First, 96-well polystyrene microtiter plates were coated with 100 μL of 10 μg/mL KD247 IgG (anti-V3 tip specific) in CBB and incubated for 1 h at 37°C followed by blocking with 175 μL 2% BSA-PBS. After washing, 50 μL HIV-1_{BAL} gp120 supernatant (diluted in ELISA buffer) was added at 1 μg/mL per well and plates were incubated at 4°C overnight. After washing, aID mAbs were added in serial dilution followed by biotinylated anti-CD4i mAbs and then plates were incubated at 37°C for 1 h. Biotinylated anti-CD4i mAb concentrations used in this assay were the concentration at which ≥95% binding to captured HIV-1_{BAL} gp120 occurred in a separate ELISA assay system. aID mAbs were added at concentrations ≥30 times in excess of that of biotinylated anti-CD4i mAbs. Horseradish peroxidase conjugated streptavidin (SA-HRP) (ThermoFisher, Cat#N100) was added (1:20 000) to wells after washing followed by incubation at 37°C for 1 h. After washing five times, 100 μL of 2,2′-azino-bis (3-ethylbenzothiazoline-6-sulfonic acid) (ABTS) substrate solution (Roche, Cat#11112597001 and 11 112 422 001) was added to each well and the OD value was measured at 405 nm.

Binding of aID mAbs to anti-CD4i and KD247 Fab

Anti-CD4i Fab were expressed in supernatants of HEK293A stable cells and purified by His 60 Ni Superflow Resin (Takara, Cat#635662) using a 6× His tag attached to the heavy chain expression plasmid [19] and KD247 Fab was purified by collecting protein A column flow-through from the digested product of IgG by immobilised papain (Thermo Scientific, Cat#20341). In this assay, wells of microtiter plate were coated with 5 μg/mL Fab in PBS (37°C for 1 h) followed by blocking with 2% BSA-PBS (37°C for 1 h). After washing, aID mAbs were added at 5 μg/mL followed by 10 times serial dilutions and incubation for 1 h at 37°C. Goat anti-human IgG Fc HRP (Invitrogen, Cat#A18817) was added (1:10 000) to each well followed by incubation at 37°C for 1 h. ABTS was added as a substrate and the OD value was measured at 405 nm.

Competitive binding inhibition assay by anti-aID mAbs (ELISA)

First, a 96-well polystyrene microtiter plate was coated with 50 μL of 10 μg/mL 4G8D IgG in CBB overnight. After washing, anti-aID mAbs and NHG were added to the top well followed by three times serial dilution in the lower wells in 50 μL ELISA buffer and incubated for 1 h. Then, 50 μL biotinylated anti-CD4i mAbs (4E9C and 17b) were added to all wells at a concentration determined by a prior assay system and incubated for 1 h. The final concentration of anti-aID mAbs/NHG in the top well was 3 μg/mL, and for 4E9C and 17b it was 0.03 and 0.3 μg/mL, respectively. Following washing, SA-HRP was added to wells at 1:20 000 dilution and after 1 h incubation and washing, ABTS was added. OD value was recorded at 405 nm.

Screening of mAbs isolated from infected subjects for gp120 binding

Monomeric HIV-1_{BAL} gp120 was captured on a microtiter plate by KD247 Fab. Following blocking with 2% BSA-PBS, Infected subjects' IgG expressing supernatants were added at ~3 μg/mL followed by three times serial dilution in the presence or absence of 2 μg/mL of recombinant human soluble CD4 (sCD4) (R&D systems, Cat# 514-CD-050/CF). Finally, binding or sCD4 mediated binding enhancement was detected by Goat anti-human IgG Fc HRP (1:10 000) and ABTS as the substrate.

Biotinylation of aID mAbs

All aID mAbs were biotinylated by EZ link NHS-LC–LC-biotin (Thermo Scientific, Cat#21343) according to the manufacturer's protocol. In short, 200 μL of 2 mg/mL antibody solution (in PBS) was mixed with 5.5 μL of 10 mM biotin reagent (in dimethylsulfoxide) and incubated for 2 h on ice. The mixture was dialyzed against PBS to get rid of excess biotin.

Binding activity of biotinylated aID mAbs to B cells from a healthy donor

PBMCs were isolated from a healthy donor by gradient centrifugation using Ficoll-Paque™ Plus and ~ 10^7 cells were stained with BV 421 mouse anti-human IgG for 40 min. After washing, cells were blocked with 1 mg/mL of NHG for 30 min and biotinylated aID mAbs were added at 20 μg/mL followed by incubation for 40 min. FITC anti-human CD19, APC/Cy7 anti-human IgM, and APC streptavidin were added to cells after washing and incubated for 40 min. After a final wash, cells were stained with 7AAD before analysis by FACS Canto II. All incubations were carried out on ice in the dark. Binding of biotinylated Abs (APC+) to 7AAD-CD19 + IgM-IgG+ cells (B lymphocytes) was analysed using FlowJo (TreeStar) software.

Binding activity of 1F4F to Env expressing cells

HEK 293 T cells were transfected with JR-FL_{L175P} and JR-FL envelope (Env) expressing plasmids. Both plasmids also expressed enhanced green fluorescent protein (EGFP). Then, 48 h post transfection, JR-FL Env expressing cells were detached and reacted to 2 μg/mL of sample (supernatant) or control IgGs for 30 min in the presence or absence of sCD4 at 2 μg/mL. JR-FL_{L175P} Env expressing cells were analysed for sample or control antibody binding in the absence of sCD4. The cells were incubated with APC-conjugated AffiniPure F(ab′)2 Fragment Goat Anti-Human IgG (H + L) (Jackson ImmunoResearch, Cat#109–136-088) at 1:200 dilution for 15 min at room temperature, and analysed using the FACSCanto II (BD Biosciences). The reactivity of the Abs was analysed after gating the EGFP+ cells using FlowJo software.

Surface plasmon resonance (SPR) analysis

After 1-ethyl-3-(3-dimethylaminopropyl) carbodiimide hydrochloride (EDC) and N-hydroxysuccinimide (NHS) mediated activation (contact time 7 min twice) of the Series S CM5 sensor chip (Cytiva, Cat#29149603) surface, 4G8D aID and NHG were immobilised in different flow cells at 20 μg/mL (contact time 5 min) followed by blocking with ethanolamine (contact time 7 min twice). EDC, NHS and ethanolamine are components of amine coupling kit (Cytiva, Cat#BR100050). Protein A spin column purified recombinant human mAbs were allowed to contact immobilised IgGs at 2 μg/mL for 1 min. The sensor chip surface was regenerated by glycine-HCl (pH 2.0) (Cytiva, Cat# BR100355). Percent binding was calculated from the absolute response unit of each sample.

Analysis of binding activity to 9J6C by AlphaLISA

Binding of recombinant human mAbs to 9J6C Fab (Expressed and purified from supernatants of transfected ExpiCHO S cells) was analysed by AlphaLISA, because of peculiar physico-chemical property of 9J6C. 4E9C (negative control) and 9J6C Fabs were incubated with anti-6× His tag coated acceptor beads (Perkin Elmer, Cat#-AL178C) for 1 h. Protein A spin column purified recombinant human mAbs and control Abs were added to the mixture and incubated for 1 h. Finally, protein A donor beads (Perkin Elmer, Cat#AS102) were added and incubated for 1 h. In a 20 μL reaction mixture, the final concentrations of Fab, acceptor beads, IgG, and donor beads were 7.5, 20, 0.5, and 20 μg/mL respectively. Percent binding was calculated from the AlphaLISA score obtained from an Enspire luminometer (Perkin Elmer).

Competitive binding inhibition assay by anti-aID mAbs (AlphaLISA)

First, 5 μL 6X His tagged 9J6C Fab and 5 μL anti-6X His tag acceptor beads were incubated in a white 384-well

assay plate for 1 h. Then, 5 μL of anti-aID mAbs or NHG were added to the previous mixture in three times serial dilution followed by addition of 5 μL of biotinylated 916B2 and the mixture was incubated for 1 h. Finally, streptavidin donor beads (Perkin Elmer, Cat#6760002S) were added and luminescence was measured by a luminometer after 1 h incubation. The final concentrations of all experimental components were as follows: 9J6C Fab = 2.5 μg/mL, anti-6X His tag acceptor beads = 20 μg/mL, anti-aID mAbs/NHG = 3 μg/mL followed by three times serial dilution, 916B2 biotin = 0.1 μg/mL, and streptavidin donor beads = 20 μg/mL.

Synthesis of peptides

Peptides were commercially synthesized by Scrum Incorporated. N-terminus biotin was conjugated during peptide synthesis.

AlphaLISA binding assay to peptides

Biotin conjugated peptides were incubated with streptavidin donor beads and anti-aID mAbs were incubated with protein A acceptor beads (Perkin Elmer, Cat#AL101C) separately for 1 h at room temperature in the dark. Both reaction mixtures were mixed together and incubated for 1 h at room temperature in the dark before taking a reading using a luminometer. Final concentrations of peptides were 10 μg/mL and that of each bead was 20 μg/mL. mAbs were tested at 3 μg/mL followed by three times serial dilutions.

Screening of antigens by phage display

A 12-mer random peptide displayed phage library Ph. D.™-12 (New England Biolabs, Cat#E8110) with a complexity of 10^9 clones was selected for this analysis. The experiment was carried out with slight modifications to the manufacturer's instructions. Briefly, for the first panning, anti-aID mAbs at 300 μg/mL (2 μM) in 0.1 M $NaHCO_3$, pH 8.6, were coated on polystyrene microtiter plate wells overnight at 4°C. After blocking with 2% BSA in tris buffered saline (TBS) for 1 h at 4°C and washing with 0.1% Tween-20 TBS (0.1% TBST), 10^{11} library phages (100-fold representation of the library) were panned on the coated wells in 100 μL 0.1% TBST for 2 h at room temperature. Following 10 washes with 0.1% TBST, bound phages were eluted by 100 μL of elution buffer (0.2 M glycine-HCl, pH 2.2 in 1 mg/mL BSA) and neutralised by 15 μL of 1 M Tris–HCl, pH 9.1. Eluted phages were amplified by infection in early log phase ER2738 *E. coli* strain and purified by PEG precipitation. Purified phages were titrated in LB/IPTG/Xgal plates. For successive panning, washed and blocked protein A-agarose resin (Thermo Scientific, Cat#20333) was used to absorb non-specific phages for 1 hour followed by panning of the absorbed phages in polypropylene microcentrifuge tubes for 2 hours. Anti-aID bound phages were captured on washed and blocked protein A-agarose and eluted after washing with 0.5% PBST. Eluted phages were neutralised and amplified as described previously. Eluates were titrated and monoclonal phages from the third panning eluate (pre-amplified) were screened for binding to target anti-aID mAbs by ELISA (see below). Clones with specific binding were sequenced to check the selection of consensus sequences. After further amplification and purification of clones with specific binding and a consensus sequence, a binding assay was performed in duplicate.

Phage ELISA

Microtiter plate wells were coated with 5 μg/mL of anti-aID mAbs or NHG or BSA. After blocking with 2% BSA-TBS for 1 h and washing, amplified phage clone supernatant (for screening) or 10^{11} purified virions (for confirmation) were added to wells followed by five times serial dilution and incubated for 1 h. Following washing with 0.5% TBST, anti-M13 phage rabbit polyclonal antibody (Invitrogen, Cat#PA1-26758) was added at 1 μg/mL and incubated for 1 hour. Binding was detected by anti-rabbit HRP conjugated antibody (Invitrogen, Cat#A16096) and ABTS. OD value was measured at 405 nm.

Quantification and statistical analyses

Data from SPR analysis, and binding and inhibition ELISA and AlphaLISA were processed by Microsoft Excel software. GraphPad Prism (Version 10.0.2) was used to prepare graphs and perform statistical analyses.

RESULTS

Isolation of aID mAbs from mice immunized with anti-CD4i mAbs

To obtain aID mAbs against anti-CD4i Abs, mice were immunized with the mAbs, 4E9C and 916B2. After five immunizations, IgM^-IgG^+B cells reactive to the immunized anti-CD4i Ab were sorted as single cells (Figure S1A), and recombinant mAbs were constructed

by the RT-PCR of IgG variable regions and cloning into human IgG expression vectors (Figure 1a). On the basis of the ability of recombinant mAbs to inhibit the binding of the corresponding anti-CD4i mAbs to HIV-1_{BAL} gp120, eight aID mAbs against 4E9C (Figure 1b) and 10 aID mAbs against 916B2 were identified (Figure 1c). These aID mAbs were classified into three groups depending on their inhibition curve patterns. A typical sigmoid curve suggests the complete blockade of the paratope of anti-CD4i mAb with high affinity. Partial and straight inhibition curves may result from partial blockade of the paratope or weaker affinity of aID mAbs to the respective anti-CD4i mAb possibly because of the existence of idiotopes outside the paratope of anti-CD4i mAb. Analysis of the inhibitory activity of the aID mAbs against a panel of anti-CD4i mAbs revealed that three anti-4E9C mAbs—4G8D, 4G5G and 2A1—cross-inhibited the binding of gp120 and anti-CD4i mAbs other than 4E9C (Figure S1B). The cross-inhibition activity was not observed for the anti-916B2 mAbs (Figure S1C).

The binding activity of aID mAbs to the corresponding anti-CD4i mAb was examined by enzyme-linked immunosorbent assay (ELISA). Among eight anti-4E9C mAbs, 4G8A and 2A1 had slightly weaker binding activity to 4E9C Fab than the others (Figure 1b). Two anti-4E9C mAbs, 4G8D and 4G5G, which had a sigmoid

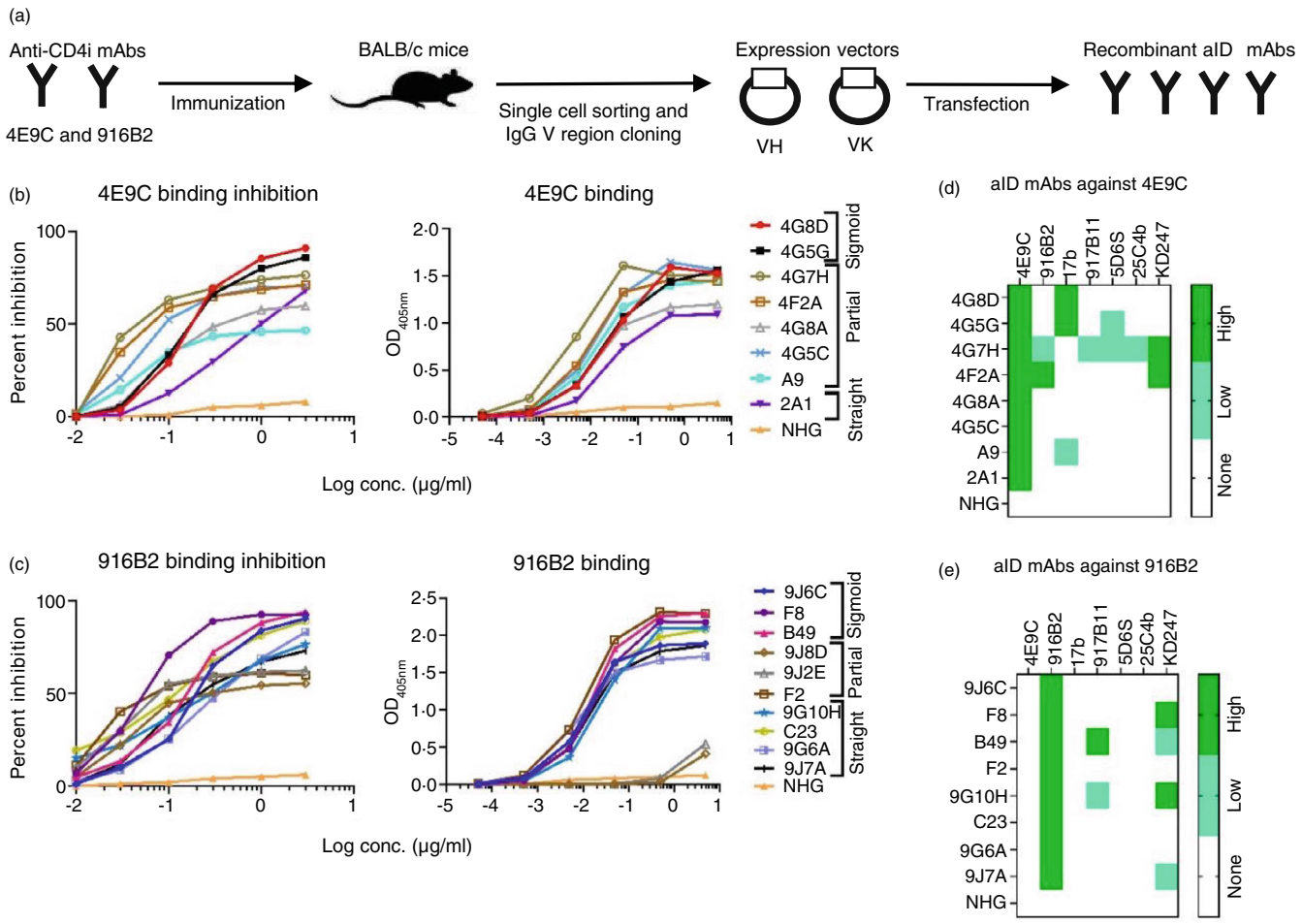

FIGURE 1 Isolation of aID mAbs from mice immunized with anti-CD4i mAbs. (a) BALB/c mice were immunized with the anti-CD4i mAbs, 4E9C and 916B2, and the recombinant mouse-human chimeric aID mAbs were produced by B cell sorting (See also Figure S1) and cloning of immunoglobulin genes. (b) Ability of aID mAbs of 4E9C to inhibit binding between 4E9C and gp120 and the binding activity of these aID mAbs to 4E9C Fab are shown. (c) Ability of aID mAbs of 916B2 to inhibit binding between 916B2 and gp120 and the binding activity of these aID mAbs to 916B2 Fab are shown. (d,e) Heatmaps summarising the binding activity, cross reactivity and specificity analyses of all aID mAbs (indicated in rows) of 4E9C and 916B2 to Fabs of the indicated anti-CD4i mAbs (in columns) by ELISA (See also Figure S1). Normal human IgG (NHG) was used as a negative control. Both 9J8D and 9J2E were excluded from these analyses because of their low-to-moderate binding activity to 916B2. An OD 405 nm value of ≤0.50 was defined as no binding, 0.51–1.00 as low binding, and 1.01–2.50 as high binding activity at the highest concentration (5 μg/mL) of aID mAbs used. All ELISA experiments were performed at least three times and representative data are shown. [Correction added on 12 January 2024, after original publication: Figure 1 was incorrect and has been replaced in this version]

inhibition pattern (Figure 1b), cross-inhibited the binding of 17b to gp120 (Figure S1B) and bound to 17b Fab (Figures 1d and S1D). In addition, 4G5G weakly cross-inhibited the binding of 5D6S to gp120, and bound to 5D6S very weakly (Figures 1d and S1B,D). Weak cross-inhibition activity was also observed for 2A1 against 916B2, and 2A1 bound to 916B2 very weakly (Figure S1B,D). A9 showed weak cross reactivity to 17b without cross-inhibition activity (Figures 1d and S1B,D). Two anti-4E9C mAbs—4G7H and 4F2A—showed binding activity to most of the anti-CD4i Fabs tested and KD247 Fab [30], the mAb against the V3 tip of HIV-1 Env (Figures 1d and S1D). These data indicated that the binding of 4G7H and 4F2A was not specific to the idiotope of 4E9C.

Among 10 anti-916B2 mAbs, eight strongly bound to 916B2 Fab (Figure 1c). However, only marginal binding activity was observed for the remaining two mAbs, 9J8D and 9J2E, which showed partial inhibition pattern (Figure 1c). Most anti-916B2 mAbs did not show any cross-reactivity to the other anti-CD4i mAbs, but B49 and 9G10H bound to 917B11 (Figures 1e and S1E). In addition, two other anti-916B2 mAbs—F8 and 9J7A—bound to anti-V3 mAb (Figures 1e and S1E), indicating the polyreactivity of these four mAbs.

Differences in the inhibitory and binding patterns suggested that various aID mAbs were induced against distinct idiotopes by the immunisation of mice. The anti-4E9C mAbs (A9, 4G7H, and 4F2A) and anti-916B2 mAbs (9J8D, 9J2E, F8, B49, 9G10H and 9J7A) were excluded from further study because they showed polyreactivity to Abs other than anti-CD4i mAbs, or had low binding or inhibition activity to the corresponding anti-CD4i Ab. The remaining aID mAbs were tested for their binding activity to live IgM-IgG+ B cells obtained from a healthy donor to further exclude polyreactivity (Figure S1F,G). From these analyses, we selected 4G8D from the anti-4E9C mAbs and 9J6C from the anti-916B2 mAbs as representative aID mAbs, which potentially mimic the β20/β21 and β2/β3 sheets of the CD4i epitope, respectively (Table S1). The mAbs—4G8D and 9J6C—strongly inhibited (Sigmoid pattern) the binding of the corresponding anti-CD4i Ab to gp120, and they did not bind to antigens other than anti-CD4i Abs.

Characterisation of mAbs reactive to aID mAbs that mimic the CD4i epitope

The representative aID mAbs against anti-CD4i mAbs—4G8D and 9J6C—were used as probes, as a mixture of two mAbs or 9J6C alone, to sort B cells expressing anti-CD4i Abs and their related clones from three HIV-1-infected subjects. IgG+ IgM-CD27+ B cells that bound to 4G8D or 9J6C were sorted as single cells (Figure S2A), and 415 mAbs were isolated from three subjects (168 from subject 1, 221 from subject 2, and 26 from subject 3). All mAbs isolated by aID mAbs were examined for binding to HIV-1_{BAL} gp120 by ELISA, and we identified one mAb reactive to gp120, 1F4F, which was isolated using a mixture of 4G8D and 9J6C as a probe (Figure 2a). Moreover, the binding of 1F4F to gp120 was significantly enhanced by human sCD4 (Figure 2a), indicating that 1F4F has a critical property of anti-CD4i mAbs. The binding of 1F4F against Env on the cell surface was much weaker than that of the anti-CD4i Ab, 4E9C, perhaps due to the masking of CD4i epitope by formation of Env trimer [31]. The binding of 1F4F was apparent by addition of sCD4, which resulted in a conformational change of Env trimer (Figures 2b and S2D). The binding of 1F4F was also observed against JR-FL_{L175P} Env mutant, which exposes the CD4i epitope in the absence of CD4 [32], but was not observed against non-transfected HEK 293 T cells (Figure S2B,C). These findings suggest that 1F4F is a typical anti-CD4i Ab, although the binding activity of 1F4F to the Env was not strong compared with that of the anti-CD4i Ab, 4E9C. Sequence analyses showed that 1F4F uses the IGHV1-69 germline gene similar to most anti-CD4i mAbs. The somatic hypermutation (SHM) in variable region of heavy chain (VH) was higher (12.5%) in 1F4F than 4E9C (7.1%) (Figure 3a). The heavy chain complementary determining region 3 (HCDR3) length of 1F4F (14 aa) was shorter than that of 4E9C (22 aa) (Figure 3a). Binding between 4E9C and 4G8D or HIV-1_{BAL} gp120 was not inhibited by 1F4F (data not shown), probably because of the low binding affinity of 1F4F compared with 4E9C.

Most anti-CD4i mAbs, including 1F4F, use the IGHV1-69 germline gene as a VH gene. The frequency of IGHV1-69 usage in mAbs isolated using 4G8D and 9J6C as probes was highest in subject 1, but was <5% in the other two subjects (Figure 2c). SPR analysis of mAbs using IGHV1-69 revealed that most mAbs isolated using a mixture of 4G8D and 9J6C, including 1F4F, bound to the 4G8D IgG, whereas the reactivity of several other mAbs was not strong and non-specific (Figure 2d). Five of the six mAbs isolated by 9J6C and two mAbs isolated using a mixture of 4G8D and 9J6C specifically bound to the 9J6C Fab, among which 1G3C, 1G5B, 1G6B and 1C6H had a higher binding activity to 9J6C than 916B2, which is the original target of 9J6C (Figure 2e). In addition, one mAb, 1G6B, which was isolated using 9J6C as a probe, bound to 4G8D and 9J6C (Figure 2d,e), indicating the presence of common idiotope on 1G6B, which is recognised by both aID mAbs.

Screening of anti-aID mAbs with the IGHV1-69 gene revealed that four anti-4G8D mAbs (1A2A, 3B5A, 1C9E and 1A5A) and two anti-9J6C mAbs (1G3C and 1G5B)

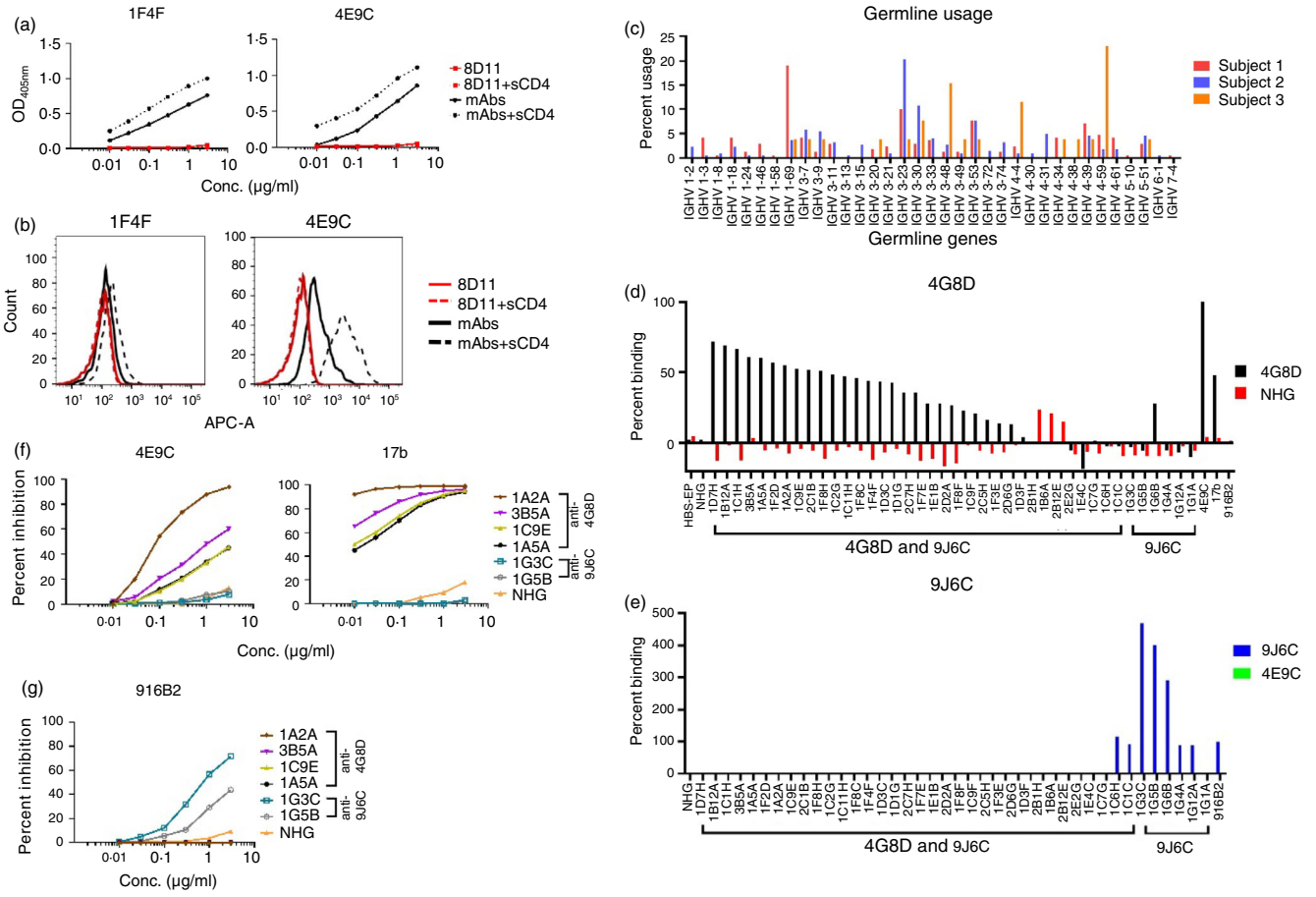

FIGURE 2 Characterisation of mAbs reactive to aID mAbs that mimic the CD4i epitope in HIV-1 infected subjects. Binding of mAb, 1F4F, to the gp120 monomer (a) and Env on the cell surface (b) was examined in the presence or absence of sCD4. The binding to gp120 monomer was analysed by ELISA using HIV-1_{BAL} gp120 as an antigen. Simple linear regression analysis showed that the effect of sCD4 was statistically significant in 1F4F ($p = 0.0495$) and 4E9C ($p = 0.0155$). The binding to Env on the cell surface was analysed by flow cytometry using 293T cells transfected with the plasmid expressing HIV-1_{JR-FL} Env. The mAbs, 4E9C and 8D11, were used as positive and negative controls, respectively. The mAb 8D11 is a mAb of unknown specificity and non-reactive to HIV-1 Env [25]. (c) Germline usage of all the mAbs isolated from three subjects is shown. (d) Anti-aID mAbs with the IGHV1-69 gene were analysed for their binding activity to aID mAb, 4G8D. The binding activity was analysed by SPR, and is shown by relative values with 4E9C as 100%. HBS-EP, NHG, and the anti-CD4i mAbs, 4E9C, 17b and 916B2 were used as controls. (e) Binding activity of anti-aID mAbs with the IGHV1-69 gene to 9J6C Fab was analysed by AlphaLISA. The binding activity is shown by relative values with 916B2 as 100%. NHG, 4E9C and 916B2 were used as controls. (f) The ability of anti-4G8D mAbs to inhibit binding and cross binding between 4G8D and 4E9C or 17b was analysed by ELISA. (g) The ability of anti-9J6C mAbs to inhibit binding between 9J6C and 916B2 was analysed by AlphaLISA. ELISA, AlphaLISA, and flow cytometry experiments were performed at least three times and representative data are shown. [Correction added on 12 January 2024, after original publication: Figure 2 was incorrect and has been replaced in this version]

inhibited binding between the corresponding aID mAb and anti-CD4i mAb (Figure S2E). The inhibition of these anti-aID mAbs was dose dependent, and all four anti-4G8D mAbs also inhibited the binding of 4G8D to 17b (Figure 2f,g). The IGHV1-69 gene usage and inhibition of binding between anti-CD4i mAbs and aID mAbs, which mimic the CD4i epitope, suggest that these anti-aID mAbs share idiotopes with anti-CD4i Abs (Table S2). However, no sequence homology was found in the CDR region of these anti-aID mAbs (Figures 3a and S3A–D). Notably, the longer HCDR3 length of anti-aID mAbs correlated with a stronger inhibition of the binding between anti-CD4i mAbs and aID mAbs in anti-4G8D and anti-9J6C mAbs (Figures 2f,g and 3a).

Anti-aID mAbs that share idiotopes with anti-CD4i mAbs bind to epitopes from the human microbiome and infectious agents

To identify antigens that anti-aID mAbs target, biopanning of phage library, which displays a 12-mer random

(a)

mAbs	Subject	Characteristics	SHM VH (%)	SHM VL (%)	HCDR3 aa sequence (Length)	LCDR3 aa sequence (Length)
1F4F	Subject 1	Gp120 binder	12.5	4.5	ADRHLGTGNYAFDI (14)	QQRSNWPTF (9)
1A2A	Subject 1	4G8D and 4E9C or 17b binding inhibitor	16.5	7.6	ATSEIVVLPAAPSQDVFDI (19)	QQYTAWPRLS (10)
3B5A	Subject 3		9.1	2.8	ARGGPAGGNYYYYYMEV (17)	QQYNSWPRT (9)
1C9E	Subject 1		6.8	4.2	AREPDYGYSYHGMDV (15)	QQYNDWPRT (9)
1A5A	Subject 1		8.1	5.6	AREDAVTTGYYMDV (14)	QHYNNWPQA (9)
4E9C	KTS376	Anti -CD4i	7.1	5.2	VGGRDNDYYDSSDISSYYAMDV (22)	QHYNNWPLLYT (11)
1G3C	Subject 1	916B2 and 9J6C binding inhibitor	5.7	4.6	AREGRSSSAGRHNYYYMDV (19)	QQYYNTPLT (9)
1G5B	Subject 1		7.1	6.6	SRADTVVTRNGFYY (14)	QESYSTPYT (9)
916B2	KTS376	Anti -CD4i	8.4	5.8	ARDSDLYCSGGSCFEI (16)	LLSYSGARV (9)

(b)

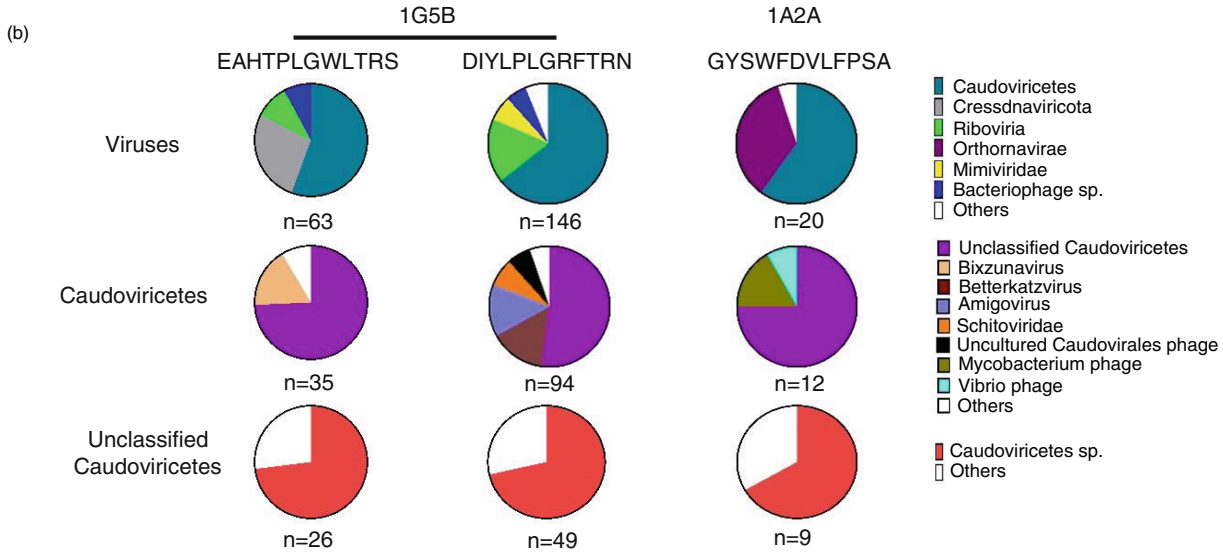

FIGURE 3 Properties of the anti-aID mAbs and results of BLAST analysis. (a) anti-aID mAbs with inhibition ability were analysed for SHM and CDR3 lengths (heavy and light chains). The effect correlated with heavy chain CDR3 length. (b) Peptide sequences obtained from consensus phage clones (See also Figure S3) selected by 1G5B and 1A2A were subject to homology search by BLAST analysis (Filters: Tax ID 10239, percent identity 100%, query coverage 50%–100%). For each peptide sequence analysed, homology to proteins from Caudoviricetes viruses were predominant. Further analysis of taxonomic classification of these viruses showed maximum homology to proteins from *Caudoviricetes* sp. under unclassified Caudoviricetes.

peptide at the N terminus of pIII, was performed using six anti-aID mAbs, which inhibited binding between the corresponding aID mAb and anti-CD4i mAb. After three rounds of biopanning, we identified two consensus peptide sequences selected by 1G5B and one sequence by 1A2A, which specifically bound to the corresponding anti-aID mAb (Figure S3E). We could not identify consensus peptide sequences reactive to other four anti-aID mAbs.

We performed a homology search for the three selected consensus peptide sequences using Basic Local Alignment Search Tool (BLAST). First, we searched for sequences with high homology to the selected 12-mer peptides. Then, virus sequences were explored in detail. For the peptide EAHTPLGWLTRS, clone 1 selected by 1G5B, we found the longest homology of 11 aa with a sequence from *Nocardioidaceae* bacterium, which was obtained from oxisol soil [33] and 8 aa homology with a sequence from a clinically significant bacterium in the marine habitat, *Vibrio vulnificus* [34, 35]. We selected proteins from these two bacteria to synthesize peptide 14 (*Nocardioidaceae*) and peptide 13 (*Vibrio vulnificus*) (Figure 4a). Two other peptides—DIYLPLGRFTRN (clone 2 selected by 1G5B) and GYSWFDVLFPSA (peptide selected by 1A2A)—did not show high sequence homology to any organism (data not shown). Because various sequences from many organisms were obtained by homology searches using short peptides, we applied filters to the search results (Tax ID 10239 designating viruses only, percent identity 100% and query coverage 50%–100%). Interestingly, all three peptides had maximum (>50%) hits to the bacteriophage *Caudoviricetes* sp. in the *Caudoviricetes* class (Figure 3b). From these results, a maximum of 7 aa homology was observed for the input sequences EAHTPLGWLTRS and GYSWFDVLFPSA with proteins of the *Caudoviricetes* class of phages from fresh water [36] or the human

(a)

Phage display		Synthesized peptides					
mAbs	sequence	Name	Sequence	Hit length (No. of aa)	Source	Organism	Accession number
1G5B	EAHTPLGWLTRS (Clone 1)	Peptide 11	Biotin -DQDILGWLTRSAEGR	7	Fresh water metagenome	Freshwater phage	ANH49402.1
		Peptide 12	Biotin -MQEIEAHTPLGLTAQ	7	Human metagenome	Caudoviricetes sp.	DAL64111.1
		Peptide 13	Biotin -KGKNTPLGWLTRILGF	8	Marine (Clinically significant bacterium)	Vibrio vulnificus	BAC97118.1
		Peptide 14	Biotin -PVAHTPLGWLTRSATI	11	Soil metagenome	Nocardioidaceae bacterium	NUR07706.1
	DIYLPLGRFTRN (Clone 2)	Peptide 21	Biotin -TKDIYLPLDNPVEMV	6	Human metagenome	Caudoviricetes sp.	DAT83460.1
		Peptide 22	Biotin -DALDNPLGRFTVEEL	6	Aquatic metagenome	Unclassified Caudoviricetes	CAB4180599.1
1A2A	GYSWFDVLFPSA	Peptide 31	Biotin -ATFASWFDVLFTVRD	7	Human metagenome	Caudoviricetes sp.	DAG12613.1

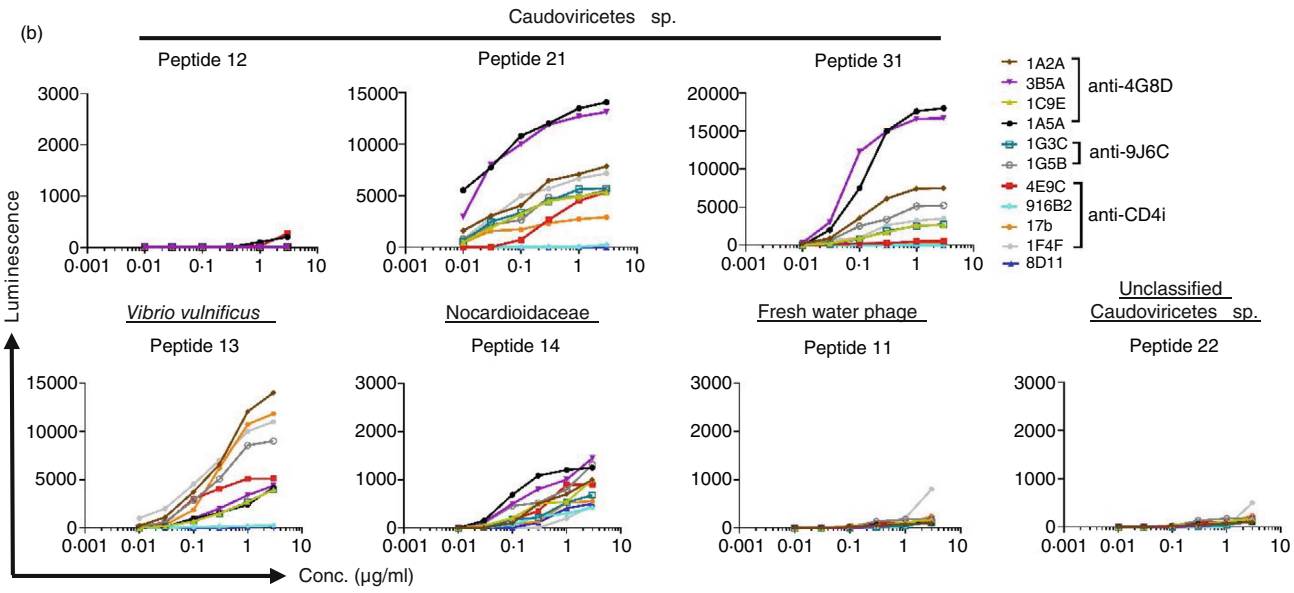

FIGURE 4 Reactivity of anti-aID mAbs sharing idiotopes with anti-CD4i mAbs to peptides from the human microbiome or infectious agents. (a) Details of the peptides synthesized from proteins of various organisms from various sources are shown. (b) Reactivity of anti-aID mAbs and anti-CD4i mAbs to biotin-conjugated peptides 12, 21, and 31 from Caudoviricetes sp., peptide 13 from Vibrio vulnificus, peptide 14 from Nocardioidaceae, peptide 11 from a fresh water phage, and peptide 22 from unclassified Caudoviricetes. Reactivity was examined by AlphaLISA using streptavidin donor beads and protein A acceptor beads, and 8D11 was used as a negative control. All experiments were performed at least three times and representative data are shown.

metagenome [37]. Peptides 11, 12 and 31 were synthesized from these protein sequences (Figure 4a). To select protein sequences for peptide synthesis, we prioritised those that spanned a maximum length of the input sequence with 2 aa overlap (Peptides 11 and 12) (Figure 4a) over those having the longest homology to the input sequence. For the DIYLPLGRFTRN input sequence, a protein with 7 aa homology (Accession number–DAU46052.1 from *Caudoviricetes* sp.) was not selected because peptides 21 and 22 together span a 10 aa region homologous to the input sequence (Figure 4a). Moreover, these two peptides had homology with proteins from phages belonging to the *Caudoviricetes* class (Figure 4a) isolated from humans [37] and the environmental metagenome [38]. For the GYSWFDVLFPSA input sequence, no overlapping sequence was found within the *Caudoviricetes* class of phages.

All synthesized peptides were examined for their reactivity to the six anti-aID mAbs and anti-CD4i mAbs, including 1F4F. Peptides 21 and 31, synthesized from proteins of *Caudoviricetes* sp. from the human metagenome, showed reactivity to most anti-aID mAbs and anti-CD4i mAbs (Figure 4b). Two anti-aID mAbs—1A5A and 3B5A—showed a stronger reaction to these peptides compared with 1G5B and 1A2A, which selected these peptides by phage display (Figure 4a,b). The reactivity to these two peptides suggests that the peptides have a similar configuration recognised by anti-CD4i mAbs and anti-aID mAbs, although the amino acid sequences were different among the peptides (Figure 4a). Moreover, mAbs reactive to the peptides from *Caudoviricetes* sp. showed a relatively high frequency of SHM, indicating maturation by repeated antigen stimulation (Figure 3a). These results suggest that a fraction of Abs, including

anti-CD4i Abs, might be induced by multiple proteins of *Caudoviricetes* sp., which have a conformation commonly contained in peptides 21 and 31.

Peptide 13 from *Vibrio vulnificus* reacted to the anti-CD4i mAbs, 4E9C, 17b and 1F4F, anti-4G8D mAbs, 1A2A, 3B5A, 1C9E and 1A5A, and anti-9J6C mAbs, 1G3C and 1G5B (Figure 4b). However, 916B2 did not react to peptide 13, although two anti-9J6C mAbs, which share the idiotope with 916B2, reacted to peptide 13. These data explain the possible role of microbial infection in the development of Abs directed against conformational epitopes.

The reactivity of mAbs to peptide 14 from *Nocardioidaceae* bacterium was very weak (Figure 4b) compared with peptide 13, although these peptides contained an eight aa sequence overlap (Figure 4a). Peptides 11 and 22 from phages in fresh water and peptide 12 from the human metagenome did not react to any mAbs tested (Figure 4b).

These data suggest that antigens from the human microbiome or infectious agents can prime and induce B cells to produce Abs sharing idiotope with anti-CD4i mAbs. A fraction of these Abs may evolve to anti-CD4i-Abs (1F4F) upon infection by HIV-1.

DISCUSSION

We used the aID tool, which was previously used for VRC01-class Abs [39], to trace priming antigens for Abs targeting a conformational CD4i epitope. We demonstrated that a fraction of Abs against the CD4i epitope of HIV-1 share idiotopes with Abs against proteins of *Caudoviricetes* sp. and *Vibrio vulnificus*. The cross-reactivity between the CD4i epitope and proteins from bacteriophages from human sources or infectious agents suggests that Abs primed by bacteriophages or infectious agents may evolve into anti-CD4i Abs during HIV-1 infection. Commensal microbes have an important role in the development of autoantibodies [40, 41] and Abs with antigen specificity [42]. Bacteriophages are abundant in human body, especially in gut, and members of *Caudovirales* order (*Podoviridae, Siphoviridae and Myoviridae*—recently classified as *Caudoviricetes* sp. by NCBI which are equivalent to *Caudovirales* sp.), which were identified as antigens targeted by Abs including anti-CD4i mAbs, are one of the major viruses in human metagenomic samples [43, 44]. Gut phageome contributes dynamically to the modulation of the immune system of the host [43–46]. Once in the circulatory system, these phages can interact with antigen presenting cells directly and contribute to the development of the immune system [43]. Moreover, this interaction can lead to the production of IgGs in contrast to the production of IgM and IgA by T cell independent [47] antigen recognition. Some of our hit sequences were from proteins of *Caudoviricetes* sp. isolated from human sources (stool, skin, mouth, nose and vagina) [37] and others belonged to environmental phages under the same (*Caudoviricetes*) class [36]. The binding activity of the examined anti-aID/anti-CD4i Abs to proteins derived from abundant bacteriophages in human metagenomic sources supports the possibility of B cell priming by these organisms, which results in high prevalence of anti-CD4i Abs in HIV-1 infected patients [48].

One of our anti-aID mAbs (1F4F) from subject 1 attained CD4i epitope binding activity and its binding activity to different peptides where applicable was comparable with other anti-CD4i mAbs (4E9C and/or 17b) (Figure 4b). Moreover, 1A5A, from the same subject, with IGHV 1–69 germline usage and that inhibits binding between 4E9C and its aID mAb 4G8D, bound to peptides from bacteriophages of human origin (possible priming antigens) with a considerably higher activity than that of 1F4F (Figure 4b). These findings suggest the possibility of antibody evolution from primed B cells.

As previously mentioned, the HIV-1 CD4i epitope is a conformational epitope, and the priming of B cells to produce anti-CD4i Abs may require a similar antigenic conformation. Peptides 21 and 13 may have a conformation similar to that of the β20/β21 sheet as indicated by 4E9C binding to these peptides (Figure 4b). However, 916B2 (β2/β3 sheet binder) did not bind to any of the peptides tested (Figure 4b), suggesting that this antibody has evolved to recognise the specific and rigid conformation of the β2/β3 sheet rather than the conformation presented by all the peptides. The detailed analysis of mAb affinity is required to understand the antigenic feature of these mAbs, but the interaction between these mAbs and peptides were too weak to measure precisely.

Vibrio vulnificus is a Gram negative bacteria from the family *Virionaceae* that is responsible for seafood related gastroenteritis, wound infection, and sepsis [35]. Infection with *Vibrio vulnificus* is limited in the subtropical seashore area, and is not common in other parts of the world. An outbreak of *Vibrio vulnificus* was reported in Kumamoto, the subject 1's geographic area [34]. Although we do not have any medical record of this subject from that time point, *Vibrio vulnificus* infection may prime B cells in this subject. During the *Vibrio vulnificus* outbreak in Kumamoto, only patients with a hepatic disorder were reported, and there might be undiagnosed individuals with mild or no symptoms of *Vibrio vulnificus* infection.

The inhibitory ability of most anti-aID mAbs correlated with HCDR3 length rather than the rate of SHM,

suggesting that V(D)J recombination in an immune repertoire [49] is important for the development and antigen specificity of these Abs. Analysis of the germline-reverted version of these mAbs will be useful to understand the role of CDRH3 and the priming potential. Our final data suggest that B cells in these repertoires may have been primed by antigens of a similar conformation presented by the complex system of the human microbiome or by the processing of antigens during infection. Similar cross reactivity of anti-gp41 Abs to gut commensal bacteria and intestinal microbiota was observed in acute HIV-1 infection [50] or after HIV-1 vaccination [51]. The evolution of anti-CD4i Abs from primed B cells may be attributed to Ab responses to other viruses. Moreover, our data may provide important information for HIV-1 vaccine design strategies to induce Abs against conformational epitopes. Stimulation of B cell populations, which are triggered by human microbiome, and their maturation to anti-HIV-1 Abs may be one of the potential strategies for HIV-1 vaccine development.

Limitations of the study

In this study, we suggest that anti-CD4i antibody-expressing B cells might be primed by antigens with a similar conformation from the human microbiome or infectious agents. Our claim is based upon shared idiotopes of the anti-aID mAbs and not antigen specificity, except for one antibody. Moreover, no structural analysis has been performed to examine the interaction between anti-aID mAbs and peptides.

AUTHOR CONTRIBUTIONS

Shuzo Matsushita and Takeo Kuwata designed the study and secured funding. Shashwata Biswas conducted patients' peripheral blood mononuclear cell sorting, cloning, recombinant IgG expression, phage display, various binding and bioinformatics analyses, and wrote the article. Hiroshi Morioka, Soichiro Yamauchi, and Kyo Okazaki designed and performed the SPR analysis. Yu Kaku and Md Zahid Hasan performed immunizations in mice and mouse spleen cell sorting.

ACKNOWLEDGEMENTS

We thank J. Ludovic Croxford, PhD, from Edanz (https://jp.edanz.com/ac) for editing a draft of this manuscript.

FUNDING INFORMATION

This work was supported in part by JSPS KAKENHI, Grant Numbers 18H0285400 and 21H02970 and by a grant for Research Program on HIV/AIDS from the Japan Agency for Medical Research and Development (JP20fk0410025h0002, JP21fk0410025h0003, JP22fk0410054h0001, and JP23fk0410054h0002).

CONFLICT OF INTEREST STATEMENT

The authors declare no conflict of interest.

DATA AVAILABILITY STATEMENT

Sequence data for antibodies have been deposited at GenBank under accession numbers OQ068368-OQ068383, OQ078767-OQ078786 and OQ078787-OQ078868. Any additional information required to reanalyze the data reported in this article is available from the lead contact upon request.

ORCID

Takeo Kuwata https://orcid.org/0000-0001-7793-6585
Md Zahid Hasan https://orcid.org/0009-0001-9639-4686
Shuzo Matsushita https://orcid.org/0000-0002-9649-8821

REFERENCES

1. Barré-Sinoussi F, Chermann JC, Rey F, Nugeyre MT, Chamaret S, Gruest J, et al. Isolation of a T-lymphotropic retrovirus from a patient at risk for acquired immune deficiency syndrome (AIDS). Science. 1983;220(4599):868–71. https://doi.org/10.1126/science.6189183
2. Haynes BF, Gilbert PB, McElrath MJ, Zolla-Pazner S, Tomaras GD, Alam SM, et al. Immune-correlates analysis of an HIV-1 vaccine efficacy trial. N Engl J Med. 2012;366(14):1275–86. https://doi.org/10.1056/NEJMoa1113425
3. Karasavvas N, Billings E, Rao M, Williams C, Zolla-Pazner S, Bailer RT, et al. The Thai phase III HIV type 1 vaccine trial (RV144) regimen induces antibodies that target conserved regions within the V2 loop of gp120. AIDS Res Hum Retroviruses. 2012;28(11):1444–57. https://doi.org/10.1089/aid.2012.0103
4. Barouch DH. Challenges in the development of an HIV-1 vaccine. Nature. 2008;455(7213):613–9. https://doi.org/10.1038/nature07352
5. McCoy LE, Weiss RA. Neutralizing antibodies to HIV-1 induced by immunization. J Exp Med. 2013;210(2):209–23. https://doi.org/10.1084/jem.20121827
6. Corey L, Gilbert PB, Tomaras GD, Haynes BF, Pantaleo G, Fauci AS. Immune correlates of vaccine protection against HIV-1 acquisition. Sci Transl Med. 2015;7(310):310rv7. https://doi.org/10.1126/scitranslmed.aac7732
7. Sattentau QJ, Dalgleish AG, Weiss RA, Beverley PCL. Epitopes of the CD4 antigen and HIV infection. Science. 1986;234(4780):1120–3. https://doi.org/10.1126/science.2430333
8. Sattentau QJ, Moore JP. Conformational changes induced in the human immunodeficiency virus envelope glycoprotein by soluble CD4 binding. J Exp Med. 1991;174(2):407–15. https://doi.org/10.1084/jem.174.2.407

9. Liu J, Bartesaghi A, Borgnia MJ, Sapiro G, Subramaniam S. Molecular architecture of native HIV-1 gp120 trimers. Nature. 2008;455(7209):109–13. https://doi.org/10.1038/nature07159
10. Guttman, M., Cupo, A., Julien, J.-P., Sanders, R. W., Wilson, I. A., Moore, J. P., & Lee, K. K. (2015). Antibody potency relates to the ability to recognize the closed, pre-fusion form of HIV env. Nat Commun, 6(1), 6144. https://doi.org/10.1038/ncomms7144
11. Wang H, Cohen AA, Galimidi RP, Gristick HB, Jensen GJ, Bjorkman PJ. Cryo-EM structure of a CD4-bound open HIV-1 envelope trimer reveals structural rearrangements of the gp120 V1V2 loop. Proc Natl Acad Sci. 2016;113(46):E7151–8. https://doi.org/10.1073/pnas.1615939113
12. Alkhatib G, Combadiere C, Broder CC, Feng Y, Kennedy PE, Murphy PM, et al. CC CKR5: a RANTES, MIP-1α, MIP-1β receptor as a fusion cofactor for macrophage-tropic HIV-1. Science. 1996;272(5270):1955–8. https://doi.org/10.1126/science.272.5270.1955
13. Dragic T, Litwin V, Allaway GP, Martin SR, Huang Y, Nagashima KA, et al. HIV-1 entry into CD4+ cells is mediated by the chemokine receptor CC-CKR-5. Nature. 1996;381(6584):667–73. https://doi.org/10.1038/381667a0
14. Weissenhorn W, Wharton SA, Calder LJ, Earl PL, Moss B, Aliprandis E, et al. The ectodomain of HIV-1 env subunit gp41 forms a soluble, alpha-helical, rod-like oligomer in the absence of gp120 and the N-terminal fusion peptide. EMBO J. 1996;15(7):1507–14.
15. Wyatt R, Sodroski J. The HIV-1 envelope glycoproteins: Fusogens, antigens, and immunogens. Science. 1998;280(5371):1884–8. https://doi.org/10.1126/science.280.5371.1884
16. Kaplan G, Roitburd-Berman A, Lewis GK, Gershoni JM. Range of CD4-bound conformations of HIV-1 gp120, as defined using conditional CD4-induced antibodies. J Virol. 2016;90(9):4481–93. https://doi.org/10.1128/JVI.03206-15
17. Thali M, Moore JP, Furman C, Charles M, Ho DD, Robinson J, et al. Characterization of conserved human immunodeficiency virus type 1 gp120 neutralization epitopes exposed upon gp120-CD4 binding. J Virol. 1993;67(7):3978–88. https://doi.org/10.1128/jvi.67.7.3978-3988.1993
18. Rizzuto CD, Wyatt R, Hernández-Ramos N, Sun Y, Kwong PD, Hendrickson WA, et al. A conserved HIV gp120 glycoprotein structure involved in chemokine receptor binding. Science. 1998;280(5371):1949–53. https://doi.org/10.1126/science.280.5371.1949
19. Tanaka K, Kuwata T, Alam M, Kaplan G, Takahama S, Valdez KPR, et al. Unique binding modes for the broad neutralizing activity of single-chain variable fragments (scFv) targeting CD4-induced epitopes. Retrovirology. 2017;14(1):44. https://doi.org/10.1186/s12977-017-0369-y
20. Naiman NE, Slyker J, Richardson BA, John-Stewart G, Nduati R, Overbaugh JM. Antibody-dependent cellular cytotoxicity targeting CD4-inducible epitopes predicts mortality in HIV-infected infants. EBioMedicine. 2019;47:257–68. https://doi.org/10.1016/j.ebiom.2019.08.072
21. Rajashekar JK, Richard J, Beloor J, Prévost J, Anand SP, Beaudoin-Bussières G, et al. Modulating HIV-1 envelope glycoprotein conformation to decrease the HIV-1 reservoir. Cell Host Microbe. 2021;29(6):904–916.e6. https://doi.org/10.1016/j.chom.2021.04.014
22. Md Zahid H, Kuwata T, Takahama S, Kaku Y, Biswas S, Matsumoto K, et al. Functional analysis of a monoclonal antibody reactive against the C1C2 of env obtained from a patient infected with HIV-1 CRF02_AG. Retrovirology. 2021;18(1):23. https://doi.org/10.1186/s12977-021-00568-y
23. Matsumoto K, Kuwata T, Tolbert WD, Richard J, Ding S, Prévost J, et al. Characterization of a novel CD4 mimetic compound YIR-821 against HIV-1 clinical isolates. J Virol. 2023;97(1):e0163822. https://doi.org/10.1128/jvi.01638-22
24. Jerne NK. Towards a network theory of the immune system. Ann Immunol. 1974;125C(1–2):373–89.
25. Ramirez Valdez KP, Kuwata T, Maruta Y, Tanaka K, Alam M, Yoshimura K, et al. Complementary and synergistic activities of anti-V3, CD4bs and CD4i antibodies derived from a single individual can cover a wide range of HIV-1 strains. Virology. 2015;475:187–203. https://doi.org/10.1016/j.virol.2014.11.011
26. Rohatgi S, Ganju P, Sehgal D. Systematic design and testing of nested (RT-)PCR primers for specific amplification of mouse rearranged/expressed immunoglobulin variable region genes from small number of B cells. J Immunol Methods. 2008;339(2):205–19. https://doi.org/10.1016/j.jim.2008.09.017
27. Tiller T, Busse CE, Wardemann H. Cloning and expression of murine Ig genes from single B cells. J Immunol Methods. 2009;350(1–2):183–93. https://doi.org/10.1016/j.jim.2009.08.009
28. Kaku Y, Kuwata T, Zahid HM, Hashiguchi T, Noda T, Kuramoto N, et al. Resistance of SARS-CoV-2 variants to neutralization by antibodies induced in convalescent patients with COVID-19. Cell Rep. 2021;36(2):109385. https://doi.org/10.1016/j.celrep.2021.109385
29. Brochet X, Lefranc M-P, Giudicelli V. IMGT/V-QUEST: the highly customized and integrated system for IG and TR standardized V-J and V-D-J sequence analysis. Nucleic Acids Res. 2008;36:W503–8. https://doi.org/10.1093/nar/gkn316
30. Matsushita S, Yoshimura K, Ramirez KP, Pisupati J, Murakami T. Passive transfer of neutralizing mAb KD-247 reduces plasma viral load in patients chronically infected with HIV-1. Aids. 2015;29(4):453–62. https://doi.org/10.1097/QAD.0000000000000570
31. Falkowska E, Le KM, Ramos A, Doores KJ, Lee JH, Blattner C, et al. Broadly neutralizing HIV antibodies define a glycan-dependent epitope on the prefusion conformation of gp41 on cleaved envelope trimers. Immunity. 2014;40(5):657–68. https://doi.org/10.1016/j.immuni.2014.04.009
32. Shibata J, Yoshimura K, Honda A, Koito A, Murakami T, Matsushita S. Impact of V2 mutations on escape from a potent neutralizing anti-V3 monoclonal antibody during in vitro selection of a primary human immunodeficiency virus type 1 isolate. J Virol. 2007;81(8):3757–68. https://doi.org/10.1128/JVI.01544-06
33. Yu J, Pavia MJ, Deem LM, Crow SE, Deenik JL, Penton CR. DNA-stable isotope probing shotgun metagenomics reveals the resilience of active microbial communities to biochar amendment in Oxisol soil. Front Microbiol. 2020;11:587972. https://doi.org/10.3389/fmicb.2020.587972
34. Matui T, Ono T, Inoue Y. An outbreak of Vibrio vulnificus infection in Kumamoto, Japan, 2001. Arch Dermatol. 2004;140(7):888–889. https://doi.org/10.1001/archderm.140.7.888

35. Leng F, Lin S, Wu W, Zhang J, Song J, Zhong M. Epidemiology, pathogenetic mechanism, clinical characteristics, and treatment of Vibrio vulnificus infection: a case report and literature review. Eur J Clin Microbiol Infect Dis. 2019;38(11): 1999–2004. https://doi.org/10.1007/s10096-019-03629-5
36. Ghai R, Mehrshad M, Mizuno CM, Rodriguez-Valera F. Metagenomic recovery of phage genomes of uncultured freshwater actinobacteria. ISME J. 2017;11(1):304–8. https://doi.org/10.1038/ismej.2016.110
37. Tisza MJ, Buck CB. A catalog of tens of thousands of viruses from human metagenomes reveals hidden associations with chronic diseases. Proc Natl Acad Sci. 2021;118(23): e2023202118. https://doi.org/10.1073/pnas.2023202118
38. Kavagutti VS, Andrei A-Ş, Mehrshad M, Salcher MM, Ghai R. Phage-centric ecological interactions in aquatic ecosystems revealed through ultra-deep metagenomics. Microbiome. 2019; 7(1):135. https://doi.org/10.1186/s40168-019-0752-0
39. Dosenovic P, Pettersson A-K, Wall A, Thientosapol ES, Feng J, Weidle C, et al. Anti-idiotypic antibodies elicit anti-HIV-1–specific B cell responses. J Exp Med. 2019;216(10):2316–30. https://doi.org/10.1084/jem.20190446
40. Riley PA. Bacteriophages in autoimmune disease and other inflammatory conditions. Med Hypotheses. 2004;62(4):493–8. https://doi.org/10.1016/j.mehy.2003.12.016
41. Chriswell ME, Lefferts AR, Clay MR, Hsu AR, Seifert J, Feser ML, et al. Clonal IgA and IgG autoantibodies from individuals at risk for rheumatoid arthritis identify an arthritogenic strain of Subdoligranulum. Sci Transl Med. 2022;14(668):eabn5166. https://doi.org/10.1126/scitranslmed.abn5166
42. Benckert J, Schmolka N, Kreschel C, Zoller MJ, Sturm A, Wiedenmann B, et al. The majority of intestinal IgA+ and IgG + plasmablasts in the human gut are antigen-specific. J Clin Invest. 2011;121(5):1946–55. https://doi.org/10.1172/JCI44447
43. Van Belleghem J, Dąbrowska K, Vaneechoutte M, Barr J, Bollyky P. Interactions between bacteriophage, bacteria, and the mammalian immune system. Viruses. 2018;11(1):10. https://doi.org/10.3390/v11010010
44. Sinha A, Maurice CF. Bacteriophages: uncharacterized and dynamic regulators of the immune system. Mediators Inflamm. 2019;2019:1–14. https://doi.org/10.1155/2019/3730519
45. Federici S, Nobs SP, Elinav E. Phages and their potential to modulate the microbiome and immunity. Cell Mol Immunol. 2021;18(4):889–904. https://doi.org/10.1038/s41423-020-00532-4
46. Popescu M, van Belleghem JD, Khosravi A, Bollyky PL. Bacteriophages and the immune system. Annu Rev Virol. 2021;8(1):415–35. https://doi.org/10.1146/annurev-virology-091919-074551
47. Allman D, Wilmore JR, Gaudette BT. The continuing story of T-cell independent antibodies. Immunol Rev. 2019;288(1):128–35. https://doi.org/10.1111/imr.12754
48. Veillette M, Coutu M, Richard J, Batraville L-A, Dagher O, Bernard N, et al. The HIV-1 gp120 CD4-bound conformation is preferentially targeted by antibody-dependent cellular cytotoxicity-mediating antibodies in sera from HIV-1-infected individuals. J Virol. 2015;89(1):545–51. https://doi.org/10.1128/JVI.02868-14
49. Chi X, Li Y, Qiu X. V(D)J recombination, somatic hypermutation and class switch recombination of immunoglobulins: mechanism and regulation. Immunology. 2020;160(3):233–47. https://doi.org/10.1111/imm.13176
50. Trama AM, Moody MA, Alam SM, Jaeger FH, Lockwood B, Parks R, et al. HIV-1 envelope gp41 antibodies can originate from terminal ileum B cells that share cross-reactivity with commensal bacteria. Cell Host Microbe. 2014;16(2):215–26. https://doi.org/10.1016/j.chom.2014.07.003
51. Williams WB, Liao H-X, Moody MA, Kepler TB, Alam SM, Gao F, et al. Diversion of HIV-1 vaccine–induced immunity by gp41-microbiota cross-reactive antibodies. Science. 2015; 349(6249):aab1253. https://doi.org/10.1126/science.aab1253

SUPPORTING INFORMATION

Additional supporting information can be found online in the Supporting Information section at the end of this article.

How to cite this article: Biswas S, Kuwata T, Yamauchi S, Okazaki K, Kaku Y, Hasan MZ, et al. Idiotopes of antibodies against HIV-1 CD4-induced epitope shared with those against microorganisms. Immunology. 2024;171(4):534–48. https://doi.org/10.1111/imm.13742